Comparison of Radar-Derived Properties of Texas Clouds Receiving One of Three Treatments: AgI Ejectable Flares or Hygroscopic Flares or No Seeding

William L. Woodley   and   Daniel Rosenfeld
Woodley Weather Consultants   Hebrew University of Jerusalem
Littleton, Colorado   Jerusalem, Israel

Abstract. Four clouds on 15 August 1996 provided an opportunity to observe and measure with radar their behaviors under various treatments: hygroscopic flares at cloud base, AgI flares near cloud top, indirect treatment with AgI ("secondary seeding") and no treatment. It was not possible to determine the expected behavior of the seeded clouds had they been left untreated, nor was it possible to reach any conclusions based on statistical analyses. Instead, the behaviors of the clouds were compared and interpreted based on physical reasoning. The cloud, which was seeded with 19 1-kgm hygroscopic flares over 43 min, was the tallest (14.9 km) and most rain productive (1,693 kilotons) of all of the clouds within scan of the radar. Based on this and other evidence, it is concluded that hygroscopic seeding may have been the most appropriate treatment for suitable clouds on this day. Because the cloud treatments were not randomized and in view of the known high natural variability of convective clouds in any region, this and other assessments presented herein must be viewed as speculative.

1. INTRODUCTION

Cloud seeding technology for rain enhancement has been under development in Texas for a number of years. The research is now being done under the acronym TEXARC (the Texas Exercise in Augmenting Rainfall through Cloud Seeding). This cloud seeding research has provided evidence for seeding-induced rain increases, which range from 100% for single clouds to 45% for rain over a floating-target area covering 2,964 km^2 (755 mi^2). The single cloud results are statistically significant at the 5% level. The area results for the 38 cases obtained to date are not statistically significant (Rosenfeld and Woodley, 1989; 1993; Woodley and Rosenfeld, 1996).

These research results, when coupled with analyses of two operational seeding efforts in Texas indicating increases in warm-season rainfall ranging between 25% and 40% (Jones, 1995; Woodley and Solak, 1990), have provided the justification for using cloud seeding in an attempt to mitigate droughts and to manage the water resources in Texas.

Not all Texas clouds are responsive to the same seeding technique and the same seeding agent. Just as physicians adapt their treatment to the needs of their patients, so too must seeding be adapted to the cloud conditions. On-top seeding with silver iodide flares as developed by the TEXARC research team of Woodley and Rosenfeld is thought to work best on vigorous convective clouds having some coalescence (Rosenfeld and Woodley, 1993). It apparently is not as effective on highly continental clouds containing very small supercooled cloud drops (Rosenfeld and Woodley, 1997). A different seeding technique and seeding agent is needed for these clouds.

Recent developments from experiments in South Africa suggest cloud-base seeding with hygroscopic flares may be effective in augmenting the rainfall from clouds that are not especially responsive to silver iodide seeding. Research by Mather and his colleagues (Mather et al., 1997) indicate that seeding with hygroscopic flares, producing tiny nuclei (average of 1 micron diameter) made up of potassium chloride and sodium chloride, produce changes in the clouds leading to earlier raindrop formation and increased rainfall.

Although there are some aspects of the results of Mather et al. (1997) that are still in question, there is reason to expect hygroscopic seeding as done in South Africa will enhance the production of raindrops in clouds and their subsequent rainfall. Confirming various aspects of the South African results now has high priority in TEXARC. Such confirmation would allow hygroscopic seeding to be used when the weather and cloud conditions are not suitable for seeding intervention with AgI.

The apparent increase in precipitation from the seeding of deep supercooled clouds at their bases with hygroscopic flares currently is thought to have been produced by the following steps (Mather et al., 1997 and personal communication with colleagues): 1) the introduction at cloud base of large and giant cloud condensation nuclei (CCN) produced by burning hygroscopic flares in racks mounted to the wings of the seeder aircraft, 2) preferential activation of the larger CCN from the flares, leading to a broadening of the cloud droplet distribution, 3) growth of the larger cloud droplets into raindrops via natural coalescence processes, in clouds which could not otherwise have "grown" raindrops through warm-rain processes, 4) the transport of the raindrops into the supercooled portion of the cloud where the raindrops

freeze due to their larger size, 5) invigoration of the cloud due to the released latent heat and growth of the frozen drops to large graupel by accretion of the cloud water, and 6) increased radar-estimated rainfall at cloud base and presumably more rainfall at the ground, when the enhanced water mass moves downward through the cloud. Several of these links in the conceptual model guiding the hygroscopic seeding experimentation have not yet been documented satisfactorily. Providing such documentation through the analysis of case studies was the goal of TEXARC 1995 and 1996.

The case studies had the following objectives: 1) detect an alteration of the cloud-base droplet spectrum as a consequence of the seeding, 2) document a seeding signature in the form of anomalously large rain drops in the supercooled portions of the clouds, 3) detect a seeding signature in the radar data in the form of unusually high reflectivities and lower first-echo heights, 4) compare and interpret the radar histories on the same day of three comparable clouds which received different treatments (i.e., hygroscopic flare seeding, silver iodide seeding (AgI) and no treatment), and 5) analyze an operational seeding case in which the same clouds were seeded concurrently with hygroscopic flares at cloud base and AgI seeding near cloud top.

Rosenfeld and Woodley (1999) have addressed objective 1, concluding that, if hygroscopic seeding affects the cloud droplet spectrum, it occurs in its tail where the few large cloud drops are not detected by the FSSP instrument. Woodley and Rosenfeld (1999a) have addressed objective 2 in a case study in which huge raindrops (up to 8mm diameter) were detected following hygroscopic flare seeding. Objectives 3 and 4 are addressed in this paper and objective 5 is

addressed in the companion to this paper (Woodley and Rosenfeld, 1999b).

2. RESULTS

Documentation of cloud development begins first on the mesoscale using the PPI and CAPPI data from the San Angelo NEXRAD radar (Figures 1a to 1n). At 2210 GMT (1710 CDT) the tiny first echoes associated with the clouds to be treated with AgI (marked by "A") and hygroscopic flares (marked by "B") can be seen about 45 km to the SSE and SSW. Twelve minutes later (7 min after initiation of hygroscopic seeding and 2 min before first AgI treatment) both echo masses had grown and intensified although maximum reflectivities had not reached 50 dBZ (Figure 1b).

At 2233 GMT the cell to the SSW receiving hygroscopic seeding was the stronger of the two with maximum reflectivities between 50 and 55 dBZ (Figure 1c). Another cell about 45 km to the WSW of the radar (marked by "C") is the unseeded cell of interest, which will be compared to the treated cells. Twelve minutes later the cell receiving hygroscopic seeding had a small reflectivity core > 55 dBZ while the cell receiving AgI seeding to the E had weakened and the unseeded cell farther W had intensified (Figure 1d).

At 2257 GMT the hyroscopically seeded cell was quite strong with maximum reflectivities > 60 dBZ. The unseeded cloud was also strong and the AgI-treated cloud was still weakening. New growth was evident to the N of the AgI parent (Figure 1e). Most of the AgI seeding took place along the upshear (North) feeders of the parent because this is where the clouds were most suitable. The directly treated cells did not grow much but debris from these cells likely provided secondary seeding for the larger parent.

By 2308 GMT (1808 CDT) the hygroscopic seeding had ceased and the cell was still quite strong on its NW edge. Cloud debris from all clouds was being exhausted to the S (Figure 1f). Both the unseeded and AgI-seeded cells had weakened although the cells to the N of the parent were growing. AgI seeding had ceased here 10 min earlier. All cells were weaker at 2320 GMT (Figure 1g). The cell that had received hygroscopic seeding was still the strongest of the three but the clouds receiving AgI had the longest N-S extent with the strongest cell on the N edge. The unseeded cloud (at "C") was the weakest of the three.

The weakening of the clouds was continuing at 2332 GMT with the cloud receiving hygroscopic flare seeding still the strongest by far (Figure 1h). This trend continued through 2343 CDT (Figure 1i) but by 0001 GMT (1901 CDT) a new echo mass had formed in the debris from the two seeded clouds (Figure 1j) and remained strong through 0031 GMT (Figures 1k and 1l). Whether the growth of this new cloud was enhanced by ingesting ice debris from the dying clouds (i.e., secondary seeding), is not known. All of the cells of interest were dead by 0111 GMT (Figures 1m and 1n).

A summation of the radar-estimated rainfalls for the duration of the cells is provided in Figure 2. The wettest area was where the clouds had received hygroscopic seeding. It had two cores of up to 75 mm of rain (3 inches). The second most productive rain area was associated with the cell that may have been seeded secondarily from cloud debris from the treated cells. Examination of the very low rain totals as evidenced by the gray-black shading suggests this cell was most affected by the debris from the AgI-seeded area since this cell appears to have been intersected by the easternmost of the two

parallel plumes streaming SSW from the two seeded areas.

The third and fourth most productive rain areas were associated with the clouds that were seeded directly with AgI and with the cloud that was never seeded. The unseeded cloud had the highest point rainfall but the rainfall from the cells treated directly with AgI covered more area. Although one can hardly claim seeding effects based on one case, we find typically the main effect of AgI seeding is to increase the areal coverage of rainfall and not its point maximum (Woodley et al., 1999c).

Figure 1b. San Angelo PPI NEXRAD radar echo presentation at 2210 GMT on 15 August 1996.

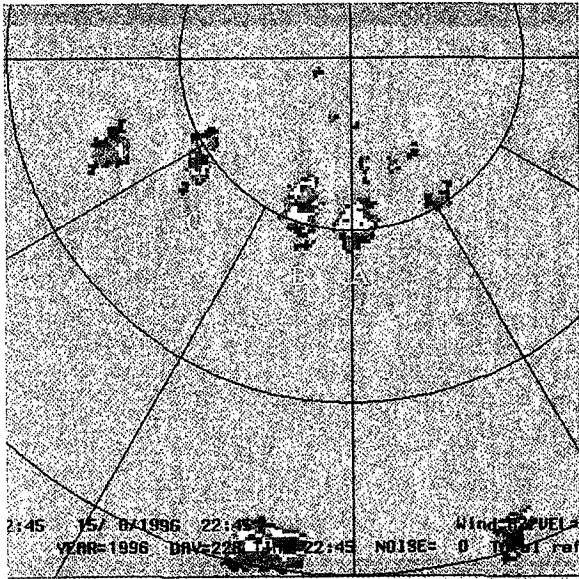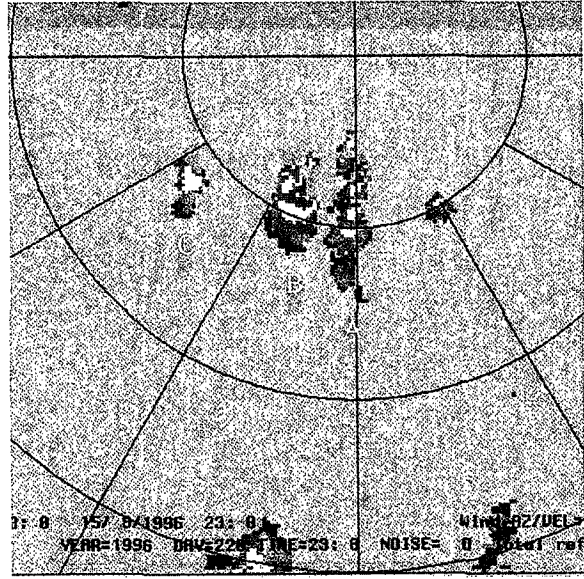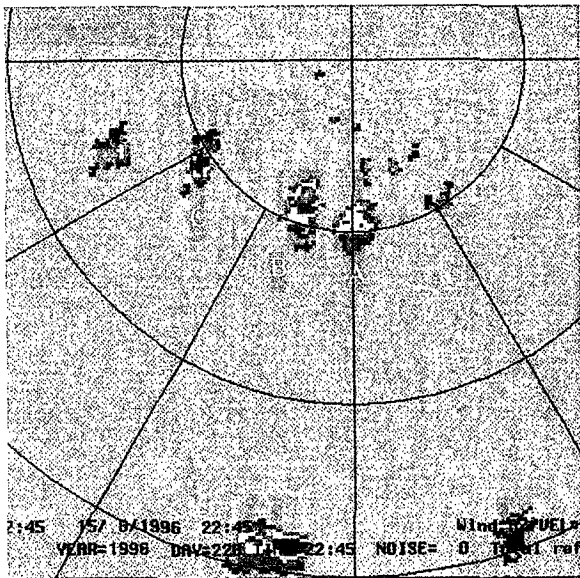Figure 1a. San Angelo PPI NEXRAD radar echo presentation at 2210 GMT on 15 August 1996. The color contours correspond to the following in dBZ: White > 60, light pink > 55, magenta > 50, orange > 45, gold > 40, yellow > 35, light green > 30, dark green > 25, light blue > 20, blue > 15, dark blue > 10, dark gray > 1, light gray > 0.
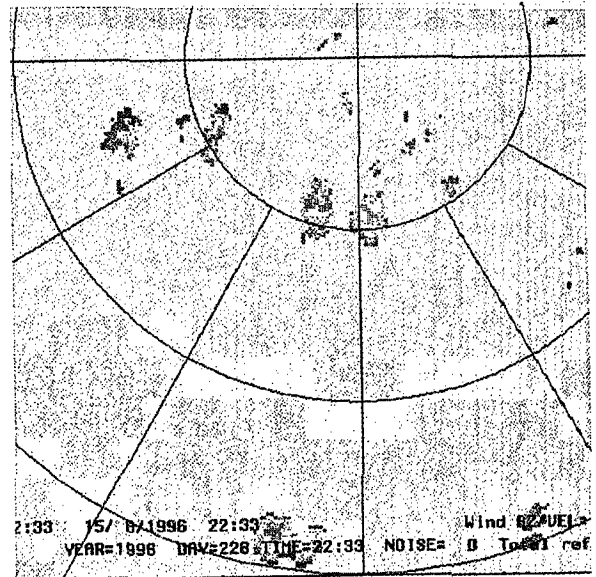
Figure 1c. San Angelo PPI NEXRAD radar echo presentation at 2233 GMT on 15 August 1996.

Figure 1d. San Angelo PPI NEXRAD radar echo presentation at 2245 GMT on 15 August 1996.

Figure 1f. San Angelo PPI NEXRAD radar echo presentation at 2308 GMT on 15 August 1996.

Figure 1e. San Angelo PPI NEXRAD radar echo presentation at 2257 GMT on 15 August 1996.
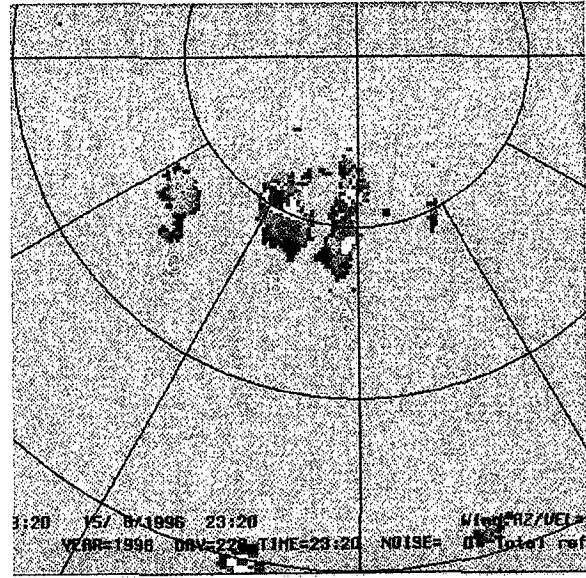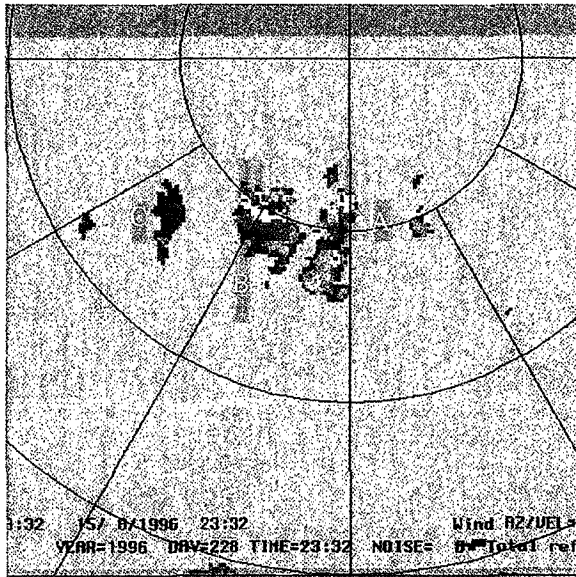

Figure 1g. San Angelo PPI NEXRAD radar echo presentation at 2320 GMT on 15 August 1996.

The next step was to focus on the lifetime properties of the individual cells as shown in Table 1. Listed are the cell number and a description of whether it received treatment directly or possibly indirectly through

secondary seeding. Following this is the cell duration (min), its maximum height (Hmax in km), reflectivity (Zmax in dBZ), area (km^2) and rain volume (10^3 m^3). The cells are listed in numerical order. The cell properties were

Figure 1h. San Angelo PPI NEXRAD radar echo presentation at 2332 GMT on 15 August 1996.
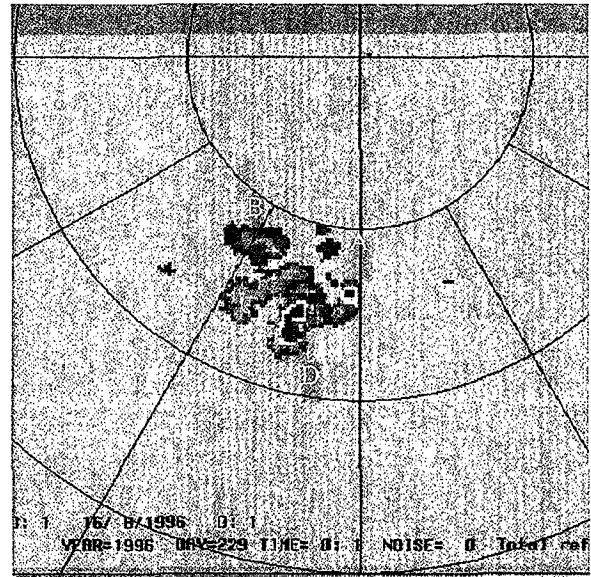

Figure 1j. San Angelo PPI NEXRAD radar echo presentation at 0001 GMT on 16 August 1996.
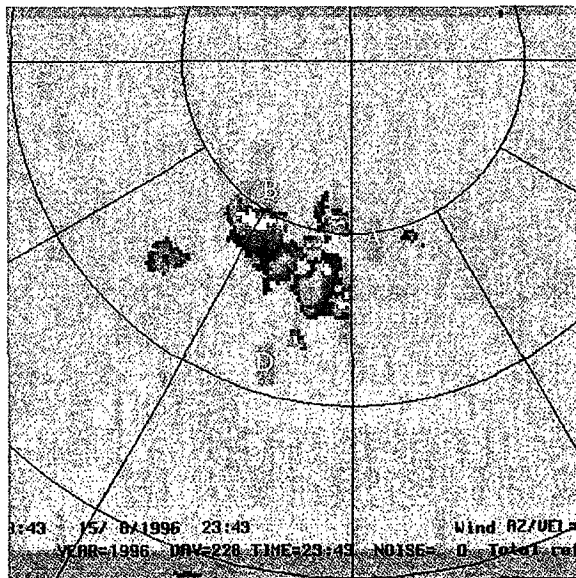

Figure 1i. San Angelo PPI NEXRAD radar echo presentation at 2343 GMT on 15 August 1996.
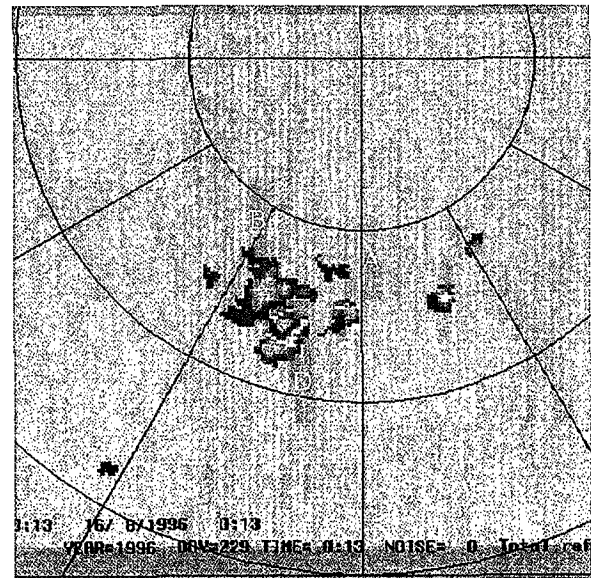

Figure 1k. San Angelo PPI NEXRAD radar echo presentation at 0013 GMT on 16 August 1996.

obtained using the tracking software of Rosenfeld (1987).

Of all the cells listed the cell receiving hygroscopic seeding cell 6826

was by far the most reflective, reaching 65 dBZ near cloud base, 60 dBZ at 7km, 50 dBZ at 11km height and a maximum echo height of 14.9 km. The AgI seeding started on small towers in cells 7390, 7771 and
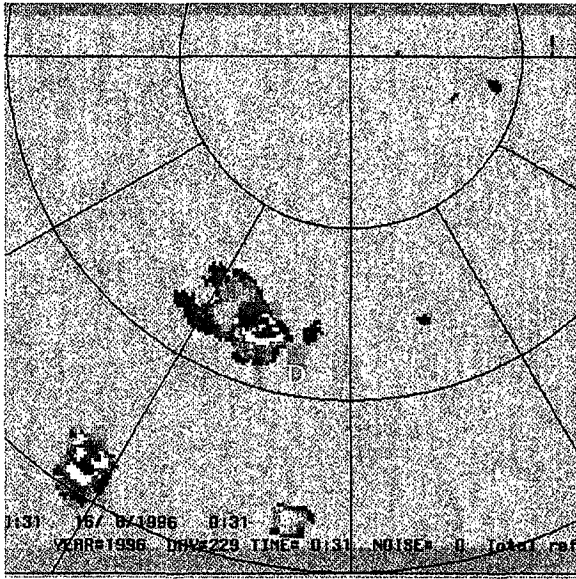
Figure 1l. San Angelo PPI NEXRAD radar echo presentation at 0031 GMT on 16 August 1996.
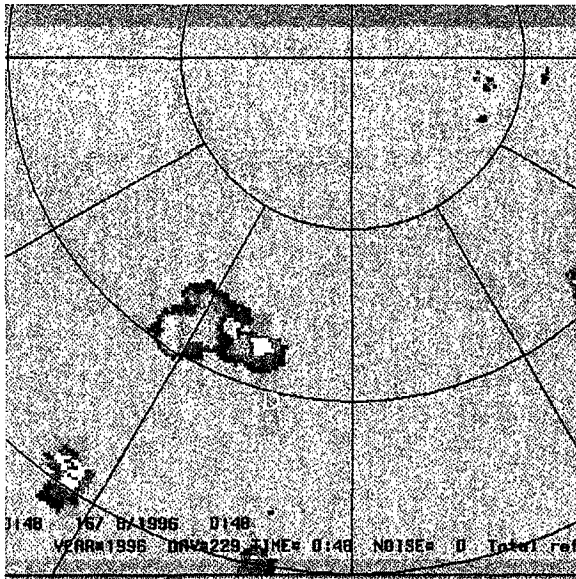

Figure 1m. San Angelo PPI NEXRAD radar echo presentation at 0048 GMT on 16 August 1996.

7976 upshear on the N edge of the main natural cloud (cell 5240). These small cells were short lived and weak. They produced downwind streamers that likely seeded cell 5240 indirectly. This cell produced 3.7 times

less rainfall than the cell receiving hygroscopic seeding and was 4.5 km shorter in stature. The unseeded cell to the W of the two seeded cells (cell 7077) was comparable in size and rain production to the indirectly AgI-seeded cell but was more reflective.

The other cell of interest (Cell #6654) appeared to form in the debris downwind of the AgI seeded cell. It produced the second most rainfall of the day and was highly reflective and covered a large area. There is no way of knowing whether the ingestion of ice debris from the earlier directly-seeded cloud ("secondary seeding") may have played any role in the development of Cell #6654.

Plots of Hmax vs. Zmax and Hmax vs. RVOL for these cells with all of the cells of the day (in green) in the background are provided in Figures 3 and 4. It is readily obvious in the plots that the cell receiving hygroscopic seeding is anomalous relative to all of the other cells. It was the tallest,
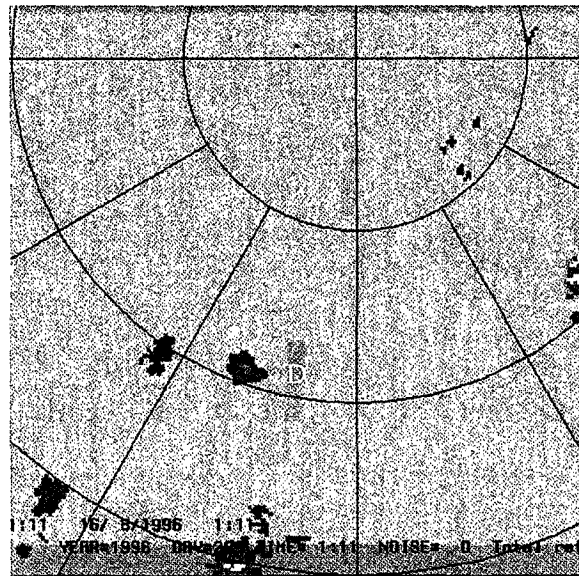

Figure 1n. San Angelo PPI NEXRAD radar echo presentation at 0111 GMT on 16 August 1996.

Table 1

Cell Lifetime Properties on 15 August 1996

Cell #	Cell Description	Duration (min)	Max Ht (km)	Max Z (mm^6/m^3)	Max Area (km^2)	RVOL (10^{3}m^3)
5240	Main AgI cell	140	10.4	52.5	102.2	453
5695	Hygro fragment	17	4.2	38.5	10.7	1
6199	Unseeded Cell	41	10.0	47.0	45.8	43
6426	Unseeded Cell	35	10.0	47.0	45.8	43
6618	Unseeded Cell	6	4.6	19.0	5.3	0
6654	Dwnd AgI Cell	187	10.8	59.5	196.0	1238
6826	Hygro Cell	111	14.9	65.0	156.1	1693
6860	Unseeded Cell	29	6.0	35.5	36.8	8
7077	Unseeded Cell	70	11.2	59.0	124.9	471
7390	AgI fragment	18	4.8	30.0	8.9	1
7771	AgI fragment	12	5.0	19.0	6.1	0
7782	Unseeded Cell	41	8.2	51.0	47.6	86
7976	AgI fragment	6	5.4	0	0	0
8644	AgI & hygro Cell	12	11.2	34.0	96.6	19
9693	Unseeded Cell	76	11.0	50.0	112.2	143
0275	Unseeded Cell	58	10.6	54.0	86.3	250

clearly the most reflective, and produced the most rainfall. It seems possible, therefore, that the hygroscopic seeding may have contributed to the development of this cloud.

The time plots of properties for the main four cells listed in Table 1 are provided in Figures 5 through 8. The plots are given in the same order as in the table. Reference to the plot for the main hygroscopic cell (*#6826*) shows the cell reached 60 dBZ about 20min after commencement of seeding and stayed above 60 dBZ for 33 min. No other cell showed such a behavior.

The cell which grew in the debris of the AgI treated cloud (#6654) also had an interesting history. It existed as a weak entity for 90min before it took off and grew into a strong storm, lasting for 90 minutes thereafter.
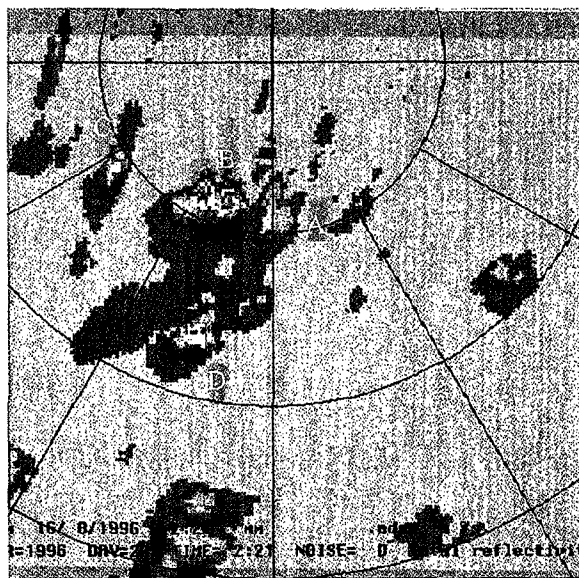

Figure 2. The radar-estimated rainfalls (mm). The color contours in mm: Pink > 100, magenta > 75, orange > 50, gold > 30, yellow > 20, light green > 15, dark green > 10, light blue > 6, blue > 4, dark blue > 2, dark gray > 1, light gray > 0.
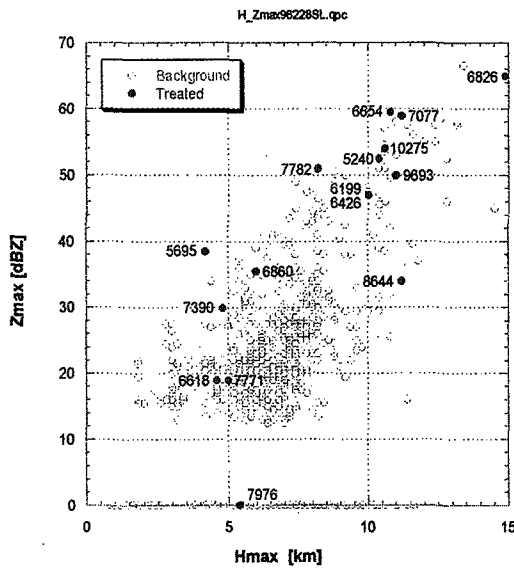
Figure 3. Scatter plot of the maximum height of the echoes (Hmax) vs. their maximum radar reflectivity (Zmax). The red points identify the direct or indirectly treated cells while the green circles correspond to the other echoes of the day within 159 km of the San Angelo NEXRAD radar.
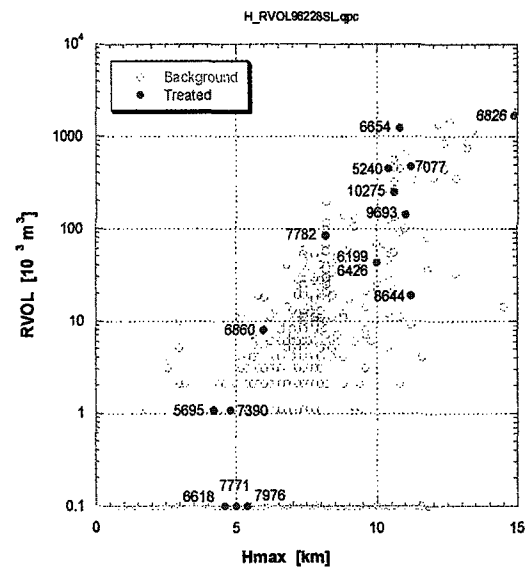
Figure 4. Scatter plot of the maximum height of the echoes (Hmax) vs. their total lifetime rain volumes (RVOL). The red points identify the direct or indirectly treated cells while the green circles correspond to the other echoes of the day within 159 km of the San Angelo NEXRAD radar.

3.0 DISCUSSION

Four clouds, which were not selected randomly for study, have been examined. All had echo tops between 5 and 6.5 km when they were treated. The one seeded with hygroscopic flares proved to be the most vigorous of the four with the highest maximum reflectivities and echo tops and the most volumetric rain production. The uncertainty is whether seeding was causal in its development.

We agree with Mather and his colleagues that hygroscopic seeding may work best when applied to supercooled convective clouds. If the seeding promotes the formation of raindrops in vigorous clouds, some of these drops will freeze when they are carried above the freezing level, because large drops freeze more readily than do small drops. This will release latent heat which will invigorate the cloud and spur additional growth while the frozen raindrops grow further into large graupel by accreting the supercooled cloud water resident in the updraft. This aspect of the hygroscopic seeding conceptual model as applied to supercooled clouds bears a strong resemblance to some of the links in the AgI seeding conceptual model. The key is the freezing of the raindrops, regardless of whether they have been produced naturally or artificially. Supercooled maritime convective clouds do this naturally and produce heavy rainfall. Seeding, whether it be hygroscopic or AgI, is intended to imitate these efficient natural processes.
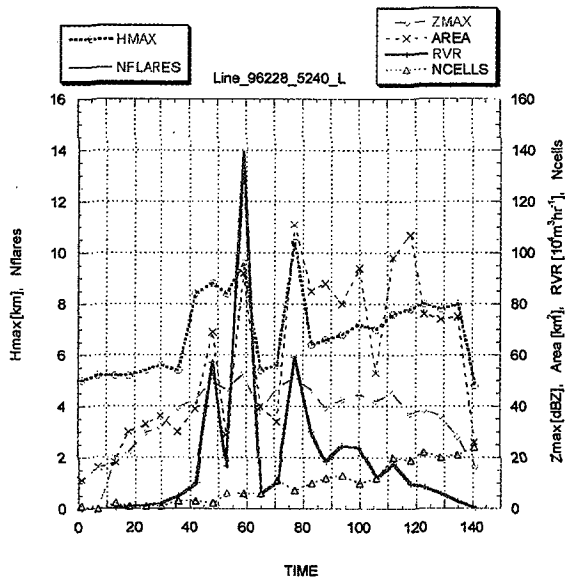
Figure 5. Line plots of the properties of cell 5240, which was seeded secondarily by ingesting AgI and/or ice particles from cells seeded directly on its upshear (North) flank. The cell properties and their units are as shown.
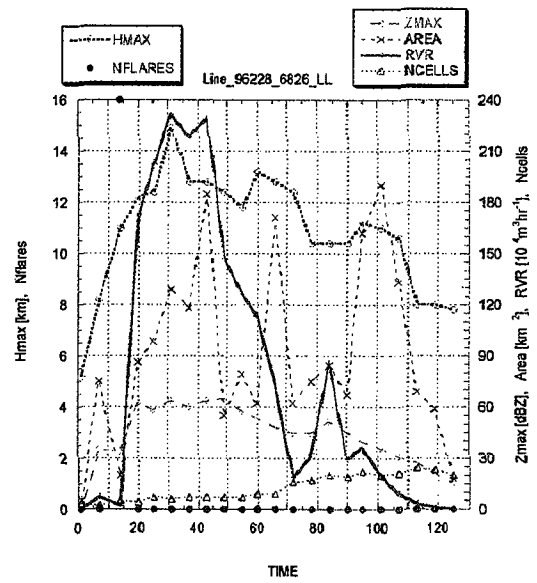

Figure 7. Same as Figure 5 but for cell 6826, which was seeded directly with 19 1-kgm hygroscopic flares at its base.
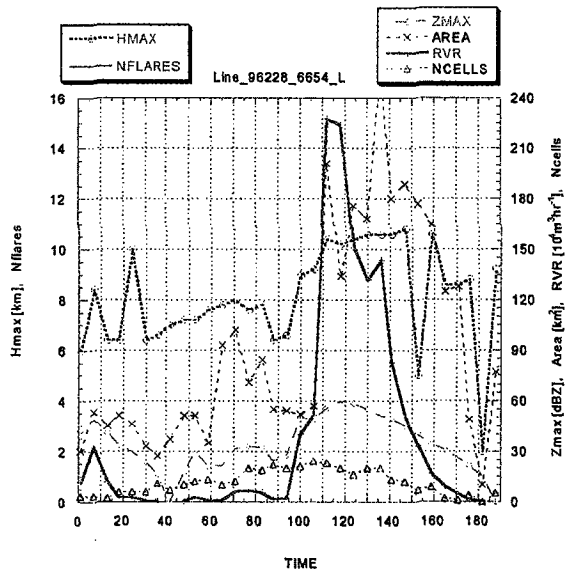

Figure 6. Same as Figure 5 but for cell 6654, which formed downwind of the directly seeded cells to its north. It appears as though cell 6654 grew through the debris from cell 5240.
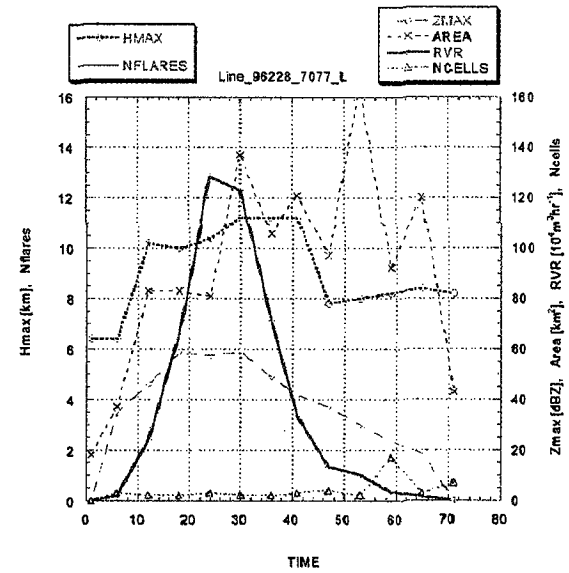

Figure 8. Same as Figure 5 but for cell 7077, which never received any treatment.

A potential problem for radar evaluation of a cloud seeding experiment, whether it be AgI seeding or hygroscopic flare seeding, is seeding-induced alteration of the raindrop spectrum causing the radar to "see" more rainfall than the non-seeded clouds than is really there. This uncertainty was addressed by Cunning (1976) in the context of the Florida Area Cumulus Experiment, which tested the efficacy of AgI flare seeding for the enhancement of rainfall. Cunning measured the size spectrum of the raindrops from AgI-seeded and non-seeded clouds and found seeding did not alter the size spectra of the raindrops below cloud base. Seeding was found to produce more ice in the AgI seeded clouds. If AgI seeding also had produced changes in the particle size spectra in the upper supercooled portion of the clouds, these alterations apparently were eliminated by adjustment of the size spectrum through droplet breakup in the large depth of cloud below the level of seeding. Thus, radar-inferred differences in rainfall from seeded and non-seeded clouds should still have been valid.

Scientists associated with hygroscopic flare seeding assume Cunning's results are applicable to their research because their clouds have depths comparable to those in Florida. There is reason now to question, however, whether Cunning's results are applicable to hygroscopic flare seeding as practiced currently. If hygroscopic seeding were to affect only the tail of the distribution and produce only a few large drops, it is possible these drops could survive intact without breakup to cloud base. Non-seeded clouds would not have such large drops and this could result in an overestimation of the effects of seeding because of the dominance of large drops on the measured radar reflectivity and on the inferred rainfall.

Both authors participated in the experiments of 15 August 1996. The first author was on the cloud-base aircraft and did the hygroscopic seeding while the second author was on the ground and watched (but without a camera!) the development of the three clouds to the SSE-SW of San Angelo. Both individuals reported independently that the rain shaft from the cloud seeded with hygroscopic flares had a different appearance from the rain shaft from the AgI-treated cloud immediately to the E of the hygroscopic cloud. The rain shaft from the AgI cloud was thick and dark, blocking completely the background, while the shaft from the hygroscopic cloud was translucent such that it was possible to see the background through it. This suggests the size distributions of the raindrops from the two clouds were different. In such case, the radar would "see" the clouds differently even if the rainfall amounts were identical.

Had the cloud physics aircraft been available on August 15, 1996, the raindrop spectra from the seeded (AgI and hygroscopic) and non-seeded clouds would have been measured and the first step taken toward resolving this issue. The best we can do is report the dramatic visual differences in the rain shafts from the AgI and hygroscopically-seeded clouds. Such impressions hardly constitute proof, however, the raindrop spectra were different and resolution of this matter must await field measurements.

These case studies also raise the issue of secondary seeding, whereby unseeded clouds ingest ice particles from previously seeded clouds. We speculate it is very important to the propagation of seeding effects in space and time long after the direct seeding has ceased. We have already documented the reality of secondary seeding on the cloud scale in Texas. One such case was obtained in TEXARC 1998. The data

show the glaciation of a cloud tower, which contained high concentrations of ice particles and no cloud water following AgI flare seeding. A new cloud tower high in cloud-water content later grew up and enveloped the old seeded tower. Aircraft penetrations of this new cloud showed high concentrations of ice (> 600/L) throughout its high cloud-water (4 gm/m^3) content region. Good photographic documentation exists for this case on the tape from the aircraft forward-looking video camera.

Assessing the impact on a field of clouds of secondary seeding, which might result also from hygroscopic flare seeding, is probably beyond our observational capabilities. When realistic cloud and mesoscale models exist, it is recommended they be used to assess the direct and indirect effects of seeding in the context of the conceptual model guiding the seeding experiments. The use of such models for the planning, evaluation and interpretation of the seeding experiments will prove to be crucial to their success.

4.0 CONCLUSIONS

The study of the four clouds receiving different treatments (AgI flares near cloud top, hygroscopic flares at cloud base, indirect treatment and no treatment) proved useful even though the treatments had not been randomized. The cloud seeded with hygroscopic flares "out performed" the other three by a large margin and was anomalous relative to all other non-seeded clouds within scan of the radar. It is concluded, therefore, that the hygroscopic seeding likely played a role in its development. The possibility exists, however, the radar-estimated rainfall from this cloud may have been overestimated due to an undocumented seeding-induced change

in its raindrop spectrum relative to the other clouds.

These case studies also raise the issue of "secondary seeding" in the development of clouds, whether seeded or not seeded. It may provide a means of propagating the effects of seeding in space and time long after seeding has ceased.

6. REFERENCES

Cunning, J.B., Jr., 1976: Comparison of the Z-R relationship for seeded and non-seeded Florida cumuli. J. Appl. Meteor., 15, 1121-1125.

Jones, R., 1995: A summary of the 1995 rain enhancement program and a review of the area rainfall and primary crop yield. Report 95-1 of the Colorado River Municipal Water District, 75pp.

Mather, G.K., D.E. Terblanche, F.E. Steffens and L. Fletcher, 1997: Results of the South African cloud seeding experiments using hygroscopic flares. J. Appl. Meteor., 36, 1433-1447.

Rosenfeld, D., 1987: Objective method for tracking and analysis of convective cells as seen by radar. J. Atmos. Sci., 4, 422-434.

Rosenfeld, D., and W. L. Woodley, 1989: Effects of cloud seeding in west Texas. J. Appl. Meteor., 28, 1050-1080.

Rosenfeld, D., and W. L. Woodley, 1993: Effects of cloud seeding in west Texas: Additional results and new insights. J. Appl. Meteor., 32, 1848-1866.

Rosenfeld, D., and W.L. Woodley, 1997: Cloud microphysical observations of relevance to the Texas cold-cloud conceptual seeding model. J. Wea. Mod., 29, 56-69.

Rosenfeld, D., and W.L. Woodley, 1999: Theoretical and Practical Considerations for Hygroscopic Seeding for Precipitation Enhancement. Manuscript excerpted from contract report from Woodley

Woodley, W.L. and M. Solak, 1990: Results of operational seeding over the watershed of San Angelo, Texas. J. Wea. Mod., 22, 30-42.

Woodley, W.L. and D. Rosenfeld, 1996: Testing cold-cloud seeding concepts in Texas and Thailand, Part I: Results in Texas to date. Presented at the 13th Conference on Planned and Inadvertent Weather Modification in Atlanta, Georgia from 28 January through 2 February 1996.

Woodley, W.L. and D. Rosenfeld, 1999a: Evaluation of TEXARC 1996. Contract report from Woodley Weather Consultants to the Texas Natural Resource Conservation Commission under Agency Order No. 582-8-104352.

Woodley, W.L. and D. Rosenfeld, 1999b: Simultaneous operational AgI and hygroscopic flare seeding in Texas: Rationale and Results. J. Wea Mod., 31, April 1999.

Woodley, W.L., D. Rosenfeld, W. Sukarnjanaset, P. Sudhikoses, S. Ruangsuttinaruparp and W. Khantiyanan, 1999c: The Thailand cold-cloud seeding experiment: 2. Results of the statistical evaluation. Proc. of 7th WMO Conf. on Wea. Mod., 16-22 Feb. 1999, Chiang Mai, Thailand.